

Salt formation affects the conformational and assembly properties of *p*-carboxylatocalix[4]arenes†Stuart Kennedy,^a Christine M. Beavers,^b Simon J. Teat^b and Scott J. Dalgarno^{*a}Cite this: *CrystEngComm*, 2014, 16, 3712Received 10th December 2013,
Accepted 25th February 2014

DOI: 10.1039/c3ce42523a

www.rsc.org/crystengcomm

The conformational properties and self-assembly behaviour of the *p*-carboxylatocalix[4]arenes, when in the presence of a pyridine template, are well understood. Salt formation with these molecules, a process driven by the introduction of an amino group to the 2-position of the pyridine template, has dramatic consequences on both building block conformation and the resulting self-assembly.

The *p*-carboxylatocalix[*n*]arenes (*p*CO₂[*n*]s, where *n* represents the number of aromatic rings in the calixarene) have received relatively little attention as molecular building blocks in supramolecular chemistry. This is surprising when one considers a) their structural relation to the *p*-sulfonato analogues which have been studied extensively,¹ b) the fact that the benzoate moiety has featured heavily in MOF formation² and c) that well-established synthons may be used to drive self-assembly with carboxylic acids.³ Despite this these molecules show great promise for exploitation in areas such as targeted self-assembly⁴ (through careful choice of synthon employed) and the formation of novel metal-organic systems.⁵ The latter can be discrete^{5a,c,d,f,h} or polymeric^{5b} in nature, and we have recently shown that these can be designed so as to specifically contain inherently cavity-containing *p*CO₂[4]s.^{5h}

The basic calix[4]arene (C[4]) framework adopts a cone conformation due to the presence of concerted H-bonding interactions at the polyphenolic lower-rim. This can be readily modulated through C[4] lower-rim alkylation to afford, amongst others, partially pinched-cone (*via* di-*O*-alkylation) and fully pinched-cone (*via* tetra-*O*-alkylation) conformers as shown

in Fig. 1A; tetra-*O*-alkylation with methyl or ethyl chains allows for conformational inversion through the C[4] annulus, and chains greater or equal to propyl in length are known to lock the molecule in the fully pinched-cone conformation.⁶ Once the desired conformer (or structurally mobile C[4] for OMe and OEt derivatives) has been synthesised, the introduction of upper-rim carboxylic acid functionality is relatively straightforward.

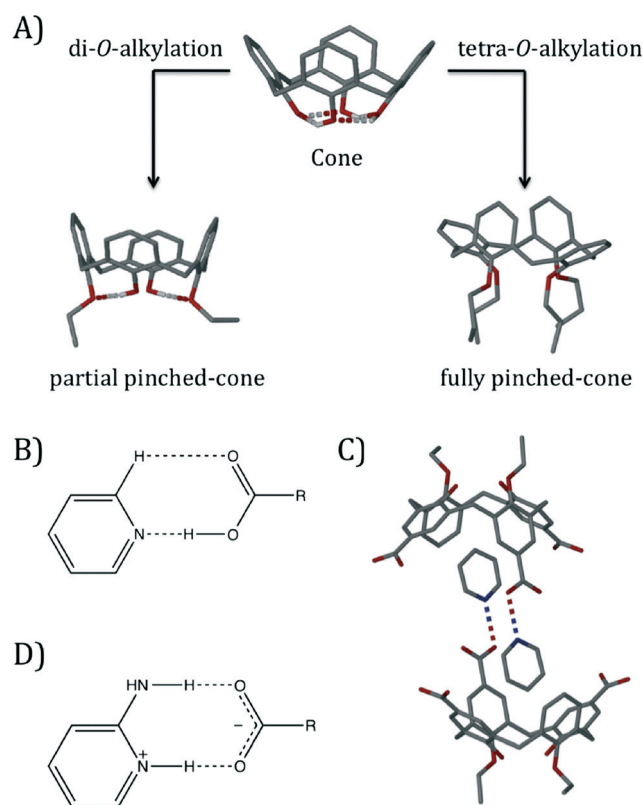


Fig. 1 A) Control over C[4] conformation by di- and tetra-*O*-alkylation at the lower-rim. B) Schematic of the Py...CO₂H heterosynthon. C) Head-to-head H-bonded capsule formed by crystallisation of a di-*O*-alkylated *p*CO₂[4] in the presence of a Py template.^{4f} D) Schematic of the 2-aminopyridinium-carboxylate heterosynthon.

^a Institute of Chemical Sciences, Heriot-Watt University, Riccarton, Edinburgh, EH14 4AS, Scotland, UK. E-mail: S.J.Dalgarno@hw.ac.uk; Fax: +44 (0)131 451 3180; Tel: +44 (0)131 451 8025

^b Lawrence Berkeley National Laboratory, 1 Cyclotron Road, MS 6R2100, Berkeley, California 94720, USA

† Electronic supplementary information (ESI) available: Crystallographic Information Files (CIFs) for 5–7 and additional figures for structural description and powder X-ray diffraction. CCDC 971748–971750. For ESI and crystallographic data in CIF or other electronic format see DOI: 10.1039/c3ce42523a



We have investigated the assembly of a range of $p\text{CO}_2[4]$ s containing two^{4b,d,f,g} or four^{4c,e} lower-rim alkyl chains in the presence of pyridine (Py), picoline and ethylpyridine templates.

In the aforementioned series of studies we found that a) the components generally formed the expected $\text{Py}\cdots\text{CO}_2\text{H}$ heterosynthon shown in Fig. 1B, b) if a cavity is present (e.g. in a lower-rim di-*O*-alkyl $p\text{CO}_2[4]$) it will be occupied by a Py or Py derivative guest template,^{4b,d,f,g} c) host-guest $p\text{CO}_2[4]$ /Py (or Py derivative) arrangements dimerise to form capsules^{4a,b,d,f,g} (Fig. 1C) and d) Py or Py derivative templates form the aforementioned heterosynthon but do not force access to the potential cavity of a lower-rim tetra-*O*-alkyl $p\text{CO}_2[4]$ (fully pinched-cone conformation, Fig. S1†).^{4c,e} Here we report interesting effects on the conformational properties of a series of tetra-*O*-alkyl $p\text{CO}_2[4]$ s, as well as their assembly preferences, once salt formation has been performed *via* introduction of an amino group to the Py template (using 2-aminopyridine, 2-AP).⁷ This well-known heterosynthon was targeted for structural comparison with related $\text{Py}\cdots\text{CO}_2\text{H}$ driven assembly of $p\text{CO}_2[4]$ s (compare Fig. 1B and D), and it was anticipated that deprotonation of the upper-rim would cause deviation from the fully pinched-cone conformation due to repulsion of CO_2^- groups. We screened salt formation in methanol between 2-aminopyridine (2-AP) and the series of *p*-carboxylato-*O*-alkylcalix[4]arenes shown in Fig. 2;† single crystals of salts formed for 1, 3 and 4, and the interesting structural features of these assemblies are described in order below.

Single crystals of the salt (5) formed between 1 and 2-AP were found to be in a monoclinic cell and structure solution was performed in the space group $P2_1/n$.† The asymmetric unit in 5 consists of one molecule of 1 (with three of four upper-rim CO_2H groups deprotonated), four 2-AP molecules (three of which are protonated, H2-AP) and two and a half methanol molecules (the half being disordered by symmetry) of crystallisation (Fig. 3). The most noticeable feature upon inspection is that 1 unexpectedly adopts a partial pinched-cone conformation; as stated above, lower-rim OMe groups allow for conformational mobility, and crystallisation of 1 from 4-picoline affords a structure in which the calixarene adopts a partial-cone conformation with inversion of one aromatic ring.^{4e,8} One of the aromatic rings of 1 in 5 is slightly splayed in comparison to the others within the framework. One H2-AP cation occupies the resulting host cavity, forming various intermolecular interactions as shown in Fig. 3; there are

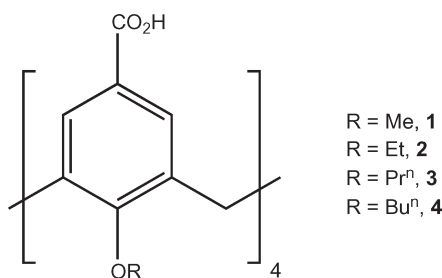


Fig. 2 Tetra-*O*-alkyl $p\text{CO}_2[4]$ s used in salt formation with 2-aminopyridine.

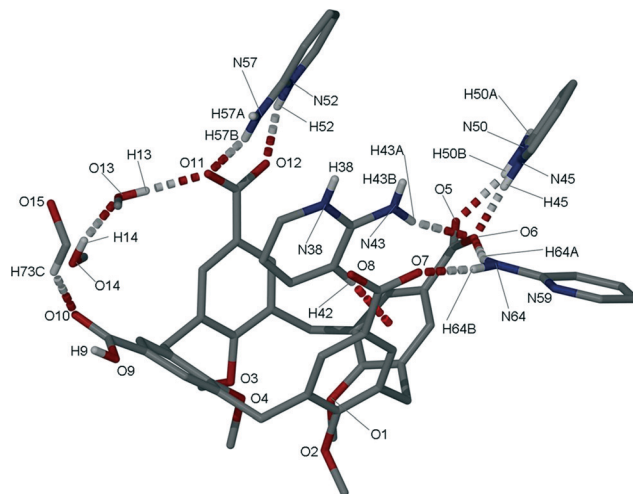


Fig. 3 Asymmetric unit found in the crystal structure of the salt (5) formed between 1 and 2-AP. H-bonding and $\text{CH}\cdots\pi$ interactions are shown as split-colour and red dashed lines respectively. Hydrogen atoms (apart from those involved in H-bonding and $\text{CH}\cdots\pi$ interactions) are omitted for clarity.

$\text{CH}\cdots\pi$ and π -stacking interactions between guest and host, occurring with respective $\text{H}[42]\cdots$ aromatic centroid and aromatic centroid \cdots aromatic centroid distances of 2.6 Å and 3.975 Å. There is also an $\text{HNH}\cdots\text{OCO}$ H-bonding interaction between the cationic guest and an upper-rim CO_2^- group of 1 with an $\text{H}[43\text{A}]\cdots\text{O}[6]$ distance of 2.2 Å. Symmetry expansion around the guest in 5 results in formation of a H-bonded head-to-head dimer/capsule as shown in Fig. 4. This occurs through formation of the targeted heterosynthon shown in Fig. 1D,⁷ with an $\text{NH}\cdots\text{OCO}$ H-bonding interaction between $\text{H}[38]$ and symmetry equivalent (s.e.) $\text{O}[7]$ ($\text{H}[38]\cdots\text{O}[7]$ s.e. distance of 1.8 Å), as well as an $\text{HNH}\cdots\text{OCO}$ H-bonding interaction between $\text{H}[43\text{B}]$ and $\text{O}[8]$ s.e. ($\text{H}[43\text{B}]\cdots\text{O}[8]$ s.e. distance of 2.0 Å). The two remaining 2-AP cations in 5 also interact with upper-rim

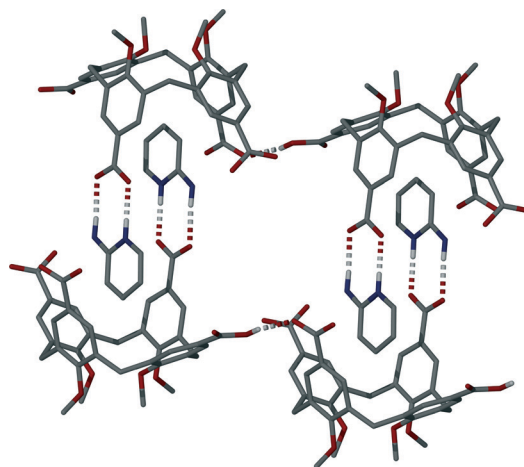


Fig. 4 H-bonding interactions (shown as split-colour dashed lines) both within and between neighbouring H-bonded head-to-head capsules in 5. Hydrogen atoms (apart from those involved in H-bonding interactions) are omitted for clarity.

CO_2^- groups of **1** through formation of the same hetero-synthon (Fig. 3); this occurs with two $\text{NH}\cdots\text{OCO}$ (respective $\text{H}[45]\cdots\text{O}[6]$ and $\text{H}[52]\cdots\text{O}[12]$ distances of 1.7 and 1.9 Å) and two $\text{HNH}\cdots\text{OCO}$ H-bonding interactions (respective $\text{H}[50\text{B}]\cdots\text{O}[5]$ and $\text{H}[57\text{B}]\cdots\text{O}[11]$ distances of 2.0 and 1.9 Å). The neutral 2-AP in the asymmetric unit interacts with two upper-rim CO_2^- groups of **1** via two $\text{HNH}\cdots\text{OCO}$ interactions with $\text{H}[64\text{A}]\cdots\text{O}[6]$ and $\text{H}[64\text{B}]\cdots\text{O}[7]$ distances of 2.1 and 2.1 Å. The three methanol molecules of crystallisation form a range of $\text{OH}\cdots\text{OCO}$ and $\text{OH}\cdots\text{O}$ H-bonding interactions; these occur between neighbouring MeOH of crystallisation, or $\text{CO}_2\text{H}/\text{CO}_2^-$ groups of **1** (Fig. 3).

Further symmetry expansion of the asymmetric unit around the splayed/protonated upper-rim CO_2H group in **1** reveals an $\text{OCO}\text{H}\cdots\text{OCO}$ H-bonding interaction to an upper-rim CO_2^- group of an s.e. molecule (Fig. 4); this unique $\text{OCO}\text{H}\cdots\text{OCO}$ interaction occurs with an $\text{H}[9]\cdots\text{O}[12]$ distance of 1.8 Å. Examination of the extended structure reveals that these capsules, linked by H-bonding interactions, pack in an anti-parallel bi-layer motif (Fig. S2†) akin to several previously reported for the Py derivative solvates of $p\text{CO}_2[4]\text{s}$.^{4e} The final noteworthy feature of **5** is that the closest distance between C atoms of the upper-rim CO_2^- groups in **1** was found to be ~7.4 Å. This is significantly greater than values typically observed for the distance between upper-rim CO_2H groups in tetra-*O*-alkyl $p\text{CO}_2[4]\text{s}$ where the lower-rim alkyl chain is greater or equal to propyl in length; the respective distances observed for **3** and **4** are ~4.1 and ~3.7 Å upon crystallisation from Py or the picolines.^{4e} Unfortunately we have been unable to crystallise **1** in a fully pinched-cone conformation to date so it is therefore not possible to make direct structural comparison between neutral and anionic forms, or draw conclusions relating to upper-rim charge repulsion and/or associated cationic guest inclusion in this particular case.

Single crystals of the salt (**6**) formed between **3** and 2-AP were found to be in a triclinic cell and structure solution was performed in the space group $P\bar{1}$.† The asymmetric unit in **6** is large and comprises two molecules of **3** (with all upper-rim CO_2H groups deprotonated), eight molecules of 2-AP (all of which are protonated and one of which is disordered over two positions), two molecules of methanol, six and a half water molecules and a disordered methanol/water of crystallisation (0.33 and 0.67 occupancies respectively). Simple inspection of **6** reveals that each calixarene cavity is occupied by a H2-AP cation, but to differing extents (Fig. 5). In the first of these there are two $\text{CH}\cdots\pi$ interactions observed between both the *meta* hydrogens of the H2-AP and aromatic rings on the anionic host (Fig. 5A); these occur with $\text{H}[92]\cdots\text{aromatic centroid}$ and $\text{H}[94]\cdots\text{aromatic centroid}$ distances of 3.1 and 2.8 Å respectively. As is the case in **5** there is concomitant $\text{HNH}\cdots\text{OCO}$ H-bonding between the cationic guest and an upper-rim CO_2^- group of the host; this occurs with an $\text{H}[95\text{B}]\cdots\text{O}[7]$ distance of 2.2 Å. Any $\text{CH}\cdots\pi$ interactions in the second host-guest arrangement can be considered to be very long (Fig. 5B),⁹ and as a result there is no evidence of analogous $\text{HNH}\cdots\text{OCO}$ H-bonding with the calixarene upper-rim. Rather

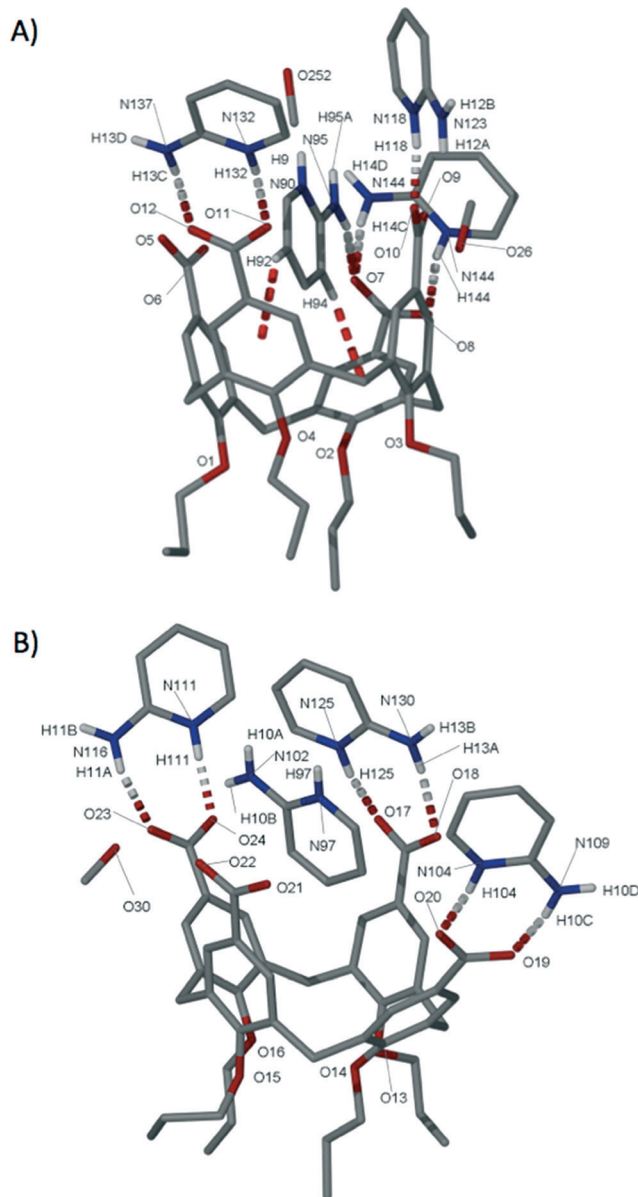


Fig. 5 Sections of the asymmetric unit in the crystal structure of the salt (**6**) formed between **3** and 2-AP. Occupation of the calixarene cavities by H2-AP cations is observed to different extents as shown in A and B; this is indicated by the presence of host-guest $\text{CH}\cdots\pi$ interactions in the former but not the latter. H-bonding and $\text{CH}\cdots\pi$ interactions are shown as split-colour and red dashed lines respectively. Hydrogen atoms (apart from those involved in H-bonding and $\text{CH}\cdots\pi$ interactions) have been omitted for clarity. Selected atoms have been labelled according to discussion.

the H2-AP cation forms an $\text{HNH}\cdots\text{O}$ H-bonding interaction with a water of crystallisation with an $\text{NH}\cdots\text{O}$ distance of 2.1 Å.

Symmetry expansion of the asymmetric unit around the upper-rim of both calixarenes reveals that, irrespective of the degree of cavity occupation by the H2-AP guests described above, formation of H-bonded head-to-head dimers akin to those found in **5** occurs via formation of the targeted hetero-synthon.⁷ In both cases this is facilitated by analogous $\text{HNH}\cdots\text{OCO}$ and $\text{NH}\cdots\text{OCO}$ H-bonding interactions as shown in Fig. 6 (capsule shown for expansion of the arrangement



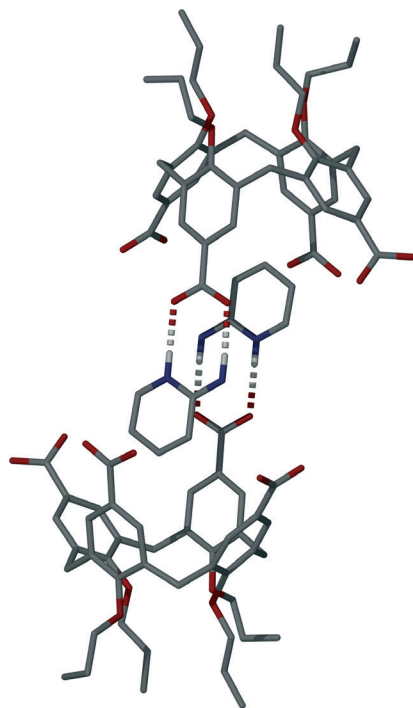


Fig. 6 One H-bonded head-to-head dimer found in the crystal structure of **6**. H-bonding interactions are shown as split-colour dashed lines. Hydrogen atoms (apart from those involved in the hydrogen-bonding interactions) are omitted for clarity.

shown in Fig. 5B). There are two $\text{NH}\cdots\text{OCO}$ hydrogen-bonding interactions between both H-bonded head-to-head dimers with respective $\text{H}[90]\cdots\text{O}[6]_{\text{s.e.}}$ and $\text{H}[97]\cdots\text{O}[22]_{\text{s.e.}}$ distances of 1.8 and 1.9 Å. Additionally there are two $\text{HNH}\cdots\text{OCO}$ H-bonding interactions with respective $\text{H}[95\text{A}]\cdots\text{O}[5]$ and $\text{H}[10\text{A}]\cdots\text{O}[20]$ distances of 2.0 and 1.9 Å.

Five of the remaining H2-AP cations in the asymmetric unit (including one of which is disordered over two positions) interact with upper-rim CO_2^- groups *via* one $\text{HNH}\cdots\text{OCO}$ and one $\text{NH}\cdots\text{OCO}$ H-bonding interaction in each case. The $\text{NH}\cdots\text{OCO}$ H-bonding interactions have distances ranging from 1.7–1.9 Å, while the $\text{HNH}\cdots\text{OCO}$ interactions range from 1.9–2.0 Å (Fig. 5). The final H2-AP cation in the asymmetric unit interacts with the remaining upper-rim CO_2^- group *via* only one $\text{NH}\cdots\text{OCO}$ H-bonding interaction with an $\text{H}[118]\cdots\text{O}[10]$ distance of 1.7 Å (Fig. 5A). The additional solvent of crystallisation (MeOH/ H_2O) forms a wide range of H-bonding interactions, but inspection shows that none appear to dictate extended assembly in an influential manner (as is the case for the cationic H2-AP template). Examination of the extended structure of **6** reveals that the components assemble as capsules within a wave-like bi-layer motif as shown in Fig. S3.†

As stated above, the average closest distance between C atoms of upper-rim CO_2H groups in **3** (when crystallised in neutral form from Py or the picolines) was found to be ~ 4.1 Å.^{4e} Examination of the analogous distances between C atoms of the upper-rim CO_2^- groups in **6** reveals that these are significantly greater with respective $\text{C}[41]\cdots\text{C}[43]$ and $\text{C}[85]\cdots\text{C}[87]$ distances of ~ 6.7 and ~ 7.1 Å (average distance of ~ 6.93 Å, Fig. 7).

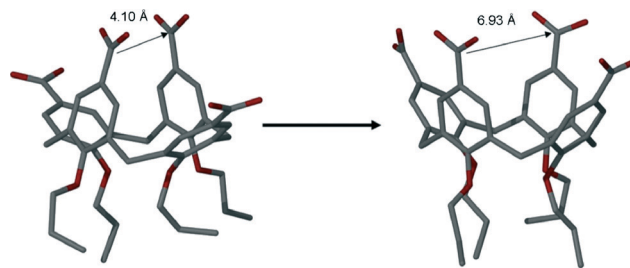


Fig. 7 Increase in the average distance between proximal upper-rim carbon atoms in neutral and tetra-anionic **3** (in **6**). Hydrogen atoms omitted for clarity.

Single crystals of the salt (**7**) formed between **4** and 2-AP were found to be in a monoclinic cell and structure solution was performed in the space group $C2/c$.† The asymmetric unit in **7** comprises one half of a molecule of **4** (with upper-rim CO_2H groups deprotonated) and two 2-AP molecules (both of which are protonated, Fig. 8).

The most noticeable feature upon inspection is that the H2-AP cations do not occupy the cavity presented by the calixarene, nor do they force access within this particular structure. One H2-AP cation in **7** forms the targeted hetero-synthon⁷ with the splayed symmetry unique upper-rim calixarene CO_2^- group *via* one $\text{NH}\cdots\text{OCO}$ and one $\text{HNH}\cdots\text{OCO}$ H-bonding interaction; this occurs with respective $\text{H}[25]\cdots\text{O}[3]$ and $\text{H}[31\text{A}]\cdots\text{O}[4]$ distances of 1.9 Å and 1.7 Å. The remaining H2-AP cation is disordered over two positions and was modelled at 50% occupancy in each. In one position this interacts with the pinched upper-rim calixarene CO_2^- group *via* one $\text{NH}\cdots\text{OCO}$ and one $\text{HNH}\cdots\text{OCO}$ hydrogen-bonding interaction; this occurs with respective $\text{H}[113]\cdots\text{O}[5]$ and $\text{H}[10\text{C}]\cdots\text{O}[6]$ distances of 1.9 Å and 2.5 Å. Symmetry expansion of the asymmetric unit around the other position reveals two $\text{HNH}\cdots\text{OCO}$ hydrogen-bonding interactions between the

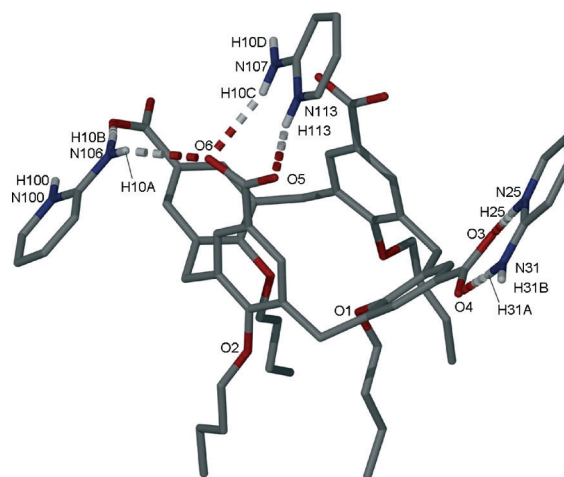


Fig. 8 Symmetry expansion of the asymmetric unit in the crystal structure of the salt (**7**) formed between **4** and 2-AP. H-bonding interactions are shown as split-colour and red dashed lines respectively. Hydrogen atoms (apart from those involved in H-bonding) have been omitted for clarity. Selected atoms have been labelled according to discussion.



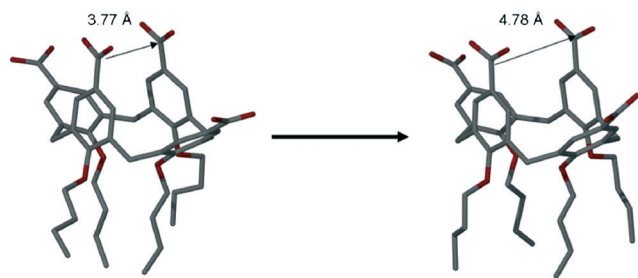


Fig. 9 Increase in the average distance between proximal upper-rim carbon atoms in neutral and tetra-anionic **4** (in **7**). Hydrogen atoms omitted for clarity.

NH₂ group on the H2-AP cation and both the splayed and pinched upper-rim CO₂[−] groups on the half-calixarene; this occurs with H[10A]...O[6] and H[10B]...O[3] distances of 2.8 and 2.3 Å. Examination of the extended structure reveals that the components pack in an anti-parallel bi-layer array as shown in Fig. S4.†

The average closest distance between C atoms of upper-rim CO₂H groups in **4** (when crystallised in neutral form from Py or the picolines) was found to be ~3.8 Å. Symmetry expansion of the asymmetric unit around the half calixarene in **7** reveals that the proximal upper-rim s.e. carbon atoms are separated by a distance of ~4.8 Å, representing a significant increase in the size of the cavity present (Fig. 9). Given that cavity occupation by a H2-AP cation is not observed, we propose that this may arise from a combination of upper-rim CO₂[−] charge repulsion and intermolecular interactions between neighbouring cations; this is difficult to state for the latter as there is disorder present in this region of the structure.

Conclusions

The *p*-carboxylatocalix[4]arenes have been shown to be versatile supramolecular building blocks in the presence of pyridine (or pyridine derivative) templates through exploitation of a) the Py...CO₂H heterosynthon and b) the availability of a cavity for template/guest occupation.^{4a,b,d,f,g} Here we have extended this template chemistry to include salt and related heterosynthon formation through the use of 2-aminopyridine. The more basic template fully deprotonated the calixarenes studied in two out of three cases, with the other forming a tri- rather than tetra-anionic building block, a feature possibly relating to poor solubility based on the short lower-rim alkyl group present. Given the observation of cavity accessibility in two cases, or the increase in cleft size relative to the neutral forms of **3** and **4** (structural comparison possible), it is reasonable to assume that the presence of the H2-AP cations markedly influences both conformational and assembly properties of the lower-rim tetra-*O*-alkyl-*p*-carboxylatocalixarenes in general. Work continues in further tailoring the assembly behaviour of these useful hosts through targeted heterosynthon formation with a view to controlling the formation of nanoscale spherical and tubular architectures.

Acknowledgements

We thank the EPSRC for financial support of this work. The Advanced Light Source is supported by the Director, Office of Science, Office of Basic Energy Sciences, of the U.S. Department of Energy under contract no. DE-AC02-05CH11231.

Notes and references

† Compounds **1–4** were prepared according to literature procedure.⁴ Synthesis of **5**: compound **1** (71 mg, 0.11 mmol) was suspended in methanol (3 ml) and excess 2-aminopyridine (309 mg, 3.3 mmol) was added. The mixture was then heated gently until the suspension became a clear solution. Slow evaporation of the solution over several hours afforded colourless single crystals suitable for diffraction studies in near-quantitative yield. Removal from the mother liquor, followed by drying and powder diffraction studies, showed that the crystals were sensitive to this procedure *via* significant differences in calculated vs. observed powder patterns. As this was the case three unit cell checks were run on single crystals taken from the sample vial in order to confirm bulk purity. These consistently corresponded to the single crystal parameters listed below for **5**. Synthesis of **6**: an analogous procedure to that followed for **5** was undertaken, using an equimolar amount of **3** as a starting material and an analogous excess ratio of 2-AP. Slow evaporation of the solution over several hours again afforded single crystals suitable for diffraction studies in near-quantitative yield. Synthesis of **7**: an analogous procedure to that followed for **5** was undertaken, using an equimolar amount of **4** as a starting material and an analogous excess ratio of 2-AP. Slow evaporation of the solution over several hours again afforded single crystals suitable for diffraction studies in near-quantitative yield. Removal from the mother liquor, followed by drying and powder diffraction studies, showed that the crystals were stable towards solvent loss *via* agreement between calculated and observed powder patterns (Fig. S5†). General crystallographic details: data for **5** and **7** were collected on a Bruker Apex II CCD Diffractometer operating at 100(2) K with synchrotron radiation ($\lambda = 0.77490$ Å). Data for **6** were collected on a Bruker Apex II CCD Diffractometer operating at 100(2) K with Mo-K α radiation ($\lambda = 0.71073$ Å). Crystal data for **5** (CCDC 971748): C₅₉H₆₇N₈O_{14.5}, $M = 1120.21$, colourless block, $0.11 \times 0.06 \times 0.04$ mm³, monoclinic, space group $P2_1/n$, $a = 12.2773(9)$, $b = 28.901(2)$, $c = 15.6350(12)$ Å, $\beta = 93.101(2)^\circ$, $V = 5539.5(7)$ Å³, $Z = 4$, $2\theta_{\max} = 50.4^\circ$, 34 609 reflections collected, 7704 unique ($R_{\text{int}} = 0.0692$). Final GooF = 1.011, $R_1 = 0.0505$, $wR_2 = 0.1342$, R indices based on 5616 reflections with $I > 2\sigma(I)$ (refinement on F^2). Crystal data for **6** (CCDC 971749): C_{130.65}H_{167.30}N₁₆O₃₄, $M = 2505.90$, colourless block, $0.40 \times 0.40 \times 0.30$ mm³, triclinic, space group $P\bar{1}$, $a = 16.5671(14)$, $b = 19.7029(17)$, $c = 20.3946(18)$ Å, $\alpha = 87.763(4)^\circ$, $\beta = 84.240(4)^\circ$, $\gamma = 77.864(3)^\circ$, $V = 6474.5(10)$ Å³, $Z = 2$, $2\theta_{\max} = 44.3^\circ$, 66 296 reflections collected, 15 780 unique ($R_{\text{int}} = 0.0360$). Final GooF = 1.893, $R_1 = 0.0809$, $wR_2 = 0.2388$, R indices based on 12 285 reflections with $I > 2\sigma(I)$ (refinement on F^2). Crystal data for **7** (CCDC 971750): C₆₈H₈₀N₈O₁₂, $M = 1201.40$, colourless block, $0.12 \times 0.06 \times 0.01$ mm³, monoclinic, space group $C2/c$, $a = 13.1086(4)$, $b = 38.2571(17)$, $c = 12.9509(6)$ Å, $\beta = 99.220(2)^\circ$, $V = 6410.9(5)$ Å³, $Z = 4$, $2\theta_{\max} = 55.3^\circ$, 34 712 reflections collected, 7377 unique ($R_{\text{int}} = 0.1098$). Final GooF = 1.389, $R_1 = 0.1289$, $wR_2 = 0.2471$, R indices based on 3229 reflections with $I > 2\sigma(I)$ (refinement on F^2).

- For relatively recent reviews on *p*-sulfonatocalix[4]arene see: J. L. Atwood, L. J. Barbour, M. J. Hardie and C. L. Raston, *Coord. Chem. Rev.*, 2001, **222**, 3; S. J. Dalgarno, J. L. Atwood and C. L. Raston, *Chem. Commun.*, 2006, 4567.
- For examples see: S. L. James, *Chem. Soc. Rev.*, 2003, **32**, 276; H. Chun, D. N. Dybtsev, H. Kim and K. Kim, *Chem.-Eur. J.*, 2005, **11**, 3521; D. J. Tranchemontagne, J. L. Mendoza-Cortes, M. O'Keeffe and O. M. Yaghi, *Chem. Soc. Rev.*, 2009, **38**, 1257; X. Lin, I. Telepeni, A. J. Blake, A. Dailly, C. M. Brown,



- J. M. Simmons, M. Zoppi, G. S. Walker, K. M. Thomas, T. J. Mays, P. Hubberstey, N. R. Champness and M. Schroder, *J. Am. Chem. Soc.*, 2009, **131**, 2159; Z. Zhang, L. Zhang, L. Wojtas, M. Eddaoudi and M. J. Zaworotko, *J. Am. Chem. Soc.*, 2012, **134**, 928; W. Morris, B. Voloskiy, S. Demir, F. Gándara, P. L. McGrier, H. Furukawa, D. Cascio, J. F. Stoddart and O. M. Yaghi, *Inorg. Chem.*, 2012, **51**, 6443; A. Schoedel, A. J. Cairns, Y. Belmabkhout, L. Wojtas, M. Mohamed, Z. Zhang, D. M. Proserpio, M. Eddaoudi and M. J. Zaworotko, *Angew. Chem., Int. Ed.*, 2013, **52**, 2902.
- 3 For example see: J. W. Steed and J. L. Atwood, in *Supramolecular Chemistry*, John Wiley and Sons, Sussex, UK, 2nd edn, 2009, ch. 8.
 - 4 (a) S. J. Dalgarno, J. E. Warren, J. Antesberger, T. E. Glass and J. L. Atwood, *New J. Chem.*, 2007, **31**, 1891; (b) S. Kennedy and S. J. Dalgarno, *Chem. Commun.*, 2009, 5275; (c) S. Kennedy, S. J. Teat and S. J. Dalgarno, *Dalton Trans.*, 2010, **39**, 384; (d) S. Kennedy, C. M. Beavers, S. J. Teat and S. J. Dalgarno, *New J. Chem.*, 2011, **35**, 28; (e) S. Kennedy, C. M. Beavers, S. J. Teat and S. J. Dalgarno, *Cryst. Growth Des.*, 2012, **12**, 679; (f) S. Kennedy, C. M. Beavers, S. J. Teat and S. J. Dalgarno, *Cryst. Growth Des.*, 2012, **12**, 688; (g) S. Kennedy, P. P. Cholewa, R. D. McIntosh and S. J. Dalgarno, *CrystEngComm*, 2013, **15**, 1520.
 - 5 (a) F. A. Cotton, P. Lei, C. Lin, C. A. Murillo, X. Wang, S. Y. Yu and Z. X. Zhang, *J. Am. Chem. Soc.*, 2004, **126**, 1518; (b) S. J. Dalgarno, K. M. Claudio-Bosque, J. E. Warren, T. E. Glass and J. L. Atwood, *Chem. Commun.*, 2008, 1410; (c) S. Kennedy, G. Karotsis, C. M. Beavers, S. J. Teat, E. K. Brechin and S. J. Dalgarno, *Angew. Chem., Int. Ed.*, 2010, **49**, 4205; (d) S. Pasquale, S. Sattin, E. C. Escudero-Adán, M. Martínez-Belmonte and J. de Mendoza, *Nat. Commun.*, 2012, **3**, 785; (e) S. P. Bew, A. D. Burrows, T. Düren, M. F. Mahon, P. Z. Moghadam, V. M. Sebesteyen and S. Thurston, *Chem. Commun.*, 2012, **48**, 4824; (f) P. P. Cholewa, C. M. Beavers, S. J. Teat and S. J. Dalgarno, *Chem. Commun.*, 2013, **49**, 3203; (g) P. P. Cholewa, C. M. Beavers, S. J. Teat and S. J. Dalgarno, *Cryst. Growth Des.*, 2013, **13**, 2703; (h) P. P. Cholewa, C. M. Beavers, S. J. Teat and S. J. Dalgarno, *Cryst. Growth Des.*, 2013, **13**, 5165.
 - 6 C. D. Gutsche, in *Calixarenes*, Royal Society of Chemistry, Cambridge, UK, 1989, ch. 4.
 - 7 J. A. Bis and M. J. Zaworotko, *Cryst. Growth Des.*, 2005, **5**, 1169; C. B. Akeröy, A. Rajbanshi, Z. J. Li and J. Desper, *CrystEngComm*, 2012, **12**, 4231.
 - 8 Compound **1** is poorly soluble in most solvents and we propose that the degree of protonation may relate to this.
 - 9 M. Nishio, *CrystEngComm*, 2004, **6**, 130.

